# Supplementary Information: A two-qubit photonic quantum processor and its application to solving systems of linear equations

Stefanie Barz[1], Ivan Kassal[2,3], Martin Ringbauer[1,*], Yannick Ole Lipp[1], Borivoje Dakić[1], Alán Aspuru-Guzik[2], Philip Walther[1]

[1] *Faculty of Physics, University of Vienna, Boltzmanngasse 5, 1090 Vienna, Austria*

[2] *Department of Chemistry and Chemical Biology, Harvard University, Cambridge MA 02138, United States*

[3] *Centre for Engineered Quantum Systems and Centre for Quantum Computing and Communication Technology, School of Mathematics and Physics, The University of Queensland, Brisbane QLD 4072, Australia*

[†] *Present address: Clarendon Laboratory, Department of Physics, University of Oxford, Parks Road, Oxford OX1 3PU, UK*

[‡] *Present address: Centre for Engineered Quantum Systems and Centre for Quantum Computing and Communication Technology, School of Mathematics and Physics, The University of Queensland, Brisbane QLD 4072, Australia*

[*] *Corresponding author: stefanie.barz@univie.ac.at*

As mentioned in the main text, the fidelity of the output state $|x\rangle$ depends on the state $R|b\rangle$ that effectively enters the control input of the first CNOT gate. Tables S1, S2, and S3 show the characterisation of the state $|x\rangle$ for various input states. Fig. S1 depicts the different input states we have chosen for our analysis.

Our analysis shows that the fidelities of the obtained output states vary from $(64.7 \pm 4.2)\%$ to $(98.1 \pm 0.9)\%$. These variations in fidelity arise due to the influence of higher-order emissions from spontaneous parametric down-conversion. These higher-order emissions can either occur when the beam passes the crystal the first time ("double-forward emission") or when the beam passes the crystal the second time ("double-backward emission"). If the input to the first CNOT gate is chosen to be $R|b\rangle = |0\rangle$ or $R|b\rangle = |1\rangle$, a double-forward emission never leads to four-photon coincidence and thus does not to a noise contribution. For all other inputs to the gate, these higher-order emissions degrade the fidelity of the output state as demonstrated in our analysis.

The "double-backward emission" can under perfect experimental conditions never lead to a fourfold coincidence because the photons can never split up due to destructive quantum interference. However, due to the visibility of the entangled Bell pairs of 0.9, this quantum interference does not work perfectly and we still have contributions of this four-photon event. About $10\%$ of our total counts arise from these events, which also influences the fidelity of the output state $|x\rangle$. The ideal output state of the gate operation can vary from being identical (setting $R|b\rangle = |1\rangle$) to being orthogonal (setting $R|b\rangle = |0\rangle$) to this of this noise contribution. This is the reason why for the input $R|b\rangle = |1\rangle$ the fidelity does not seem to be affected—the noise cannot be distinguished from the signal. The influence of the double-backward emission increases for the other input states and reaches a maximum for $R|b\rangle = |0\rangle$. This results in a lower fidelity for the input state $|0\rangle$than for the input state $|1\rangle$.

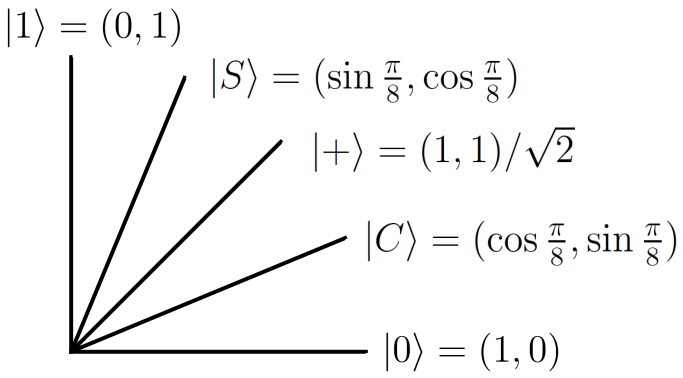


FIG. S1: The figure shows the different states $R|b\rangle$ which we have chosen as input states to our circuit.

| State $R\|b\rangle$ | Fidelity | Density Matrix |
|---|---|---|
| $\|1\rangle$ | $0.957 \pm 0.010$ | 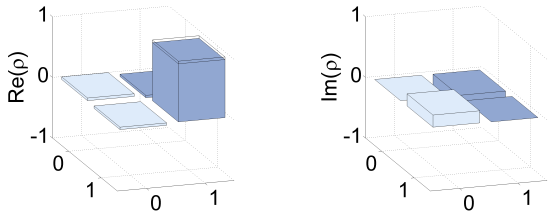 |
| $\|S\rangle$ | $0.717 \pm 0.044$ | 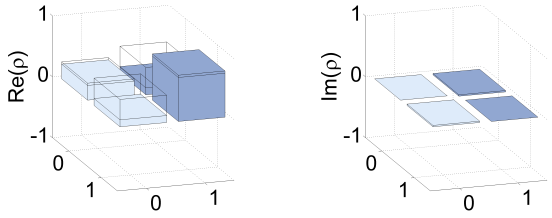 |
| $\|+\rangle$ | $0.778 \pm 0.031$ | 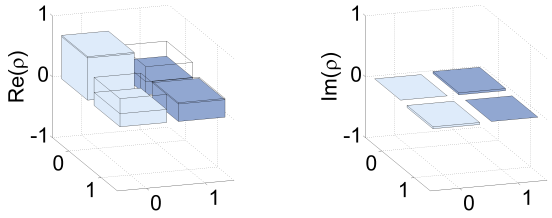 |
| $\|C\rangle$ | $0.821 \pm 0.030$ | 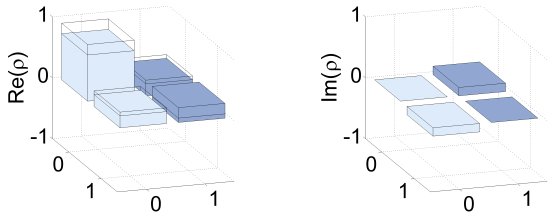 |
| $\|0\rangle$ | $0.780 \pm 0.046$ | 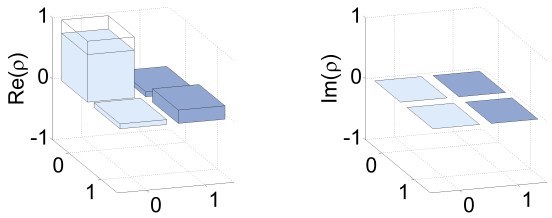 |

TABLE S1: The table shows the fidelities and density matrices of the output state $|x\rangle$ for different input states $R|b\rangle$. The eigenvalues of the matrix $A$ were chosen to be $\Lambda_1$, and $R = \mathbf{I}$.

| State $R\|b\rangle$ | Fidelity | Density Matrix |
|---|---|---|
| $\|1\rangle$ | $0.961 \pm 0.013$ | 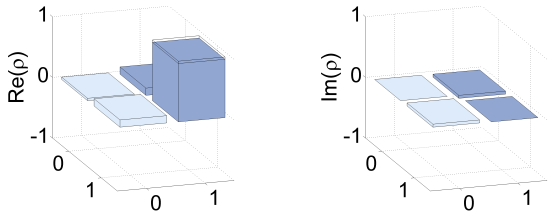 |
| $\|S\rangle$ | $0.647 \pm 0.042$ | 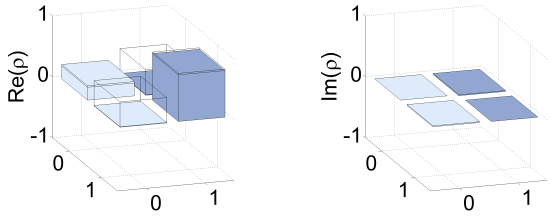 |
| $\|+\rangle$ | $0.773 \pm 0.027$ | 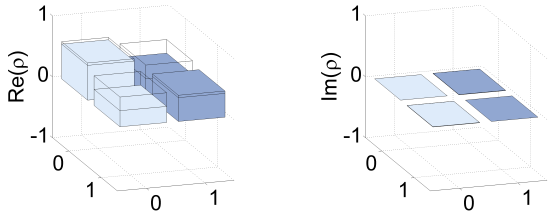 |



TABLE S2: The table shows the fidelities and density matrices of the output state $|x\rangle$ for different input states $R|b\rangle$. The eigenvalues of the matrix $A$ were chosen to be $\Lambda_2$, and $R = \mathbf{I}$.

| State $R\|b\rangle$ | Fidelity | Density Matrix |
|---|---|---|
| $\|1\rangle$ | $0.981 \pm 0.009$ | 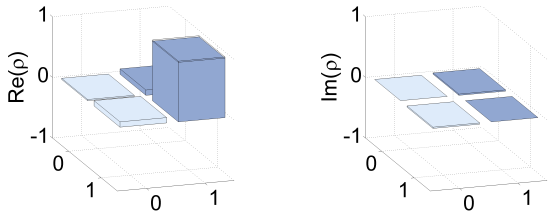 |
| $\|S\rangle$ | $0.729 \pm 0.040$ | 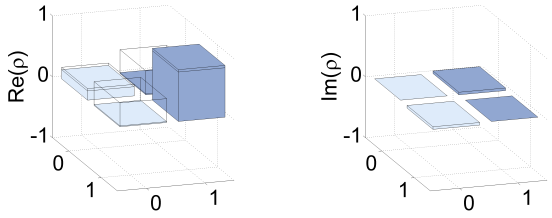 |
| $\|+\rangle$ | $0.832 \pm 0.031$ | 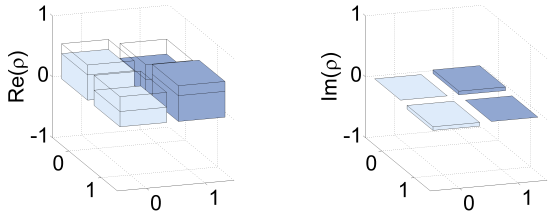 |



TABLE S3: The table shows the fidelities and density matrices of the output state $|x\rangle$ for different input states $R|b\rangle$. The eigenvalues of the matrix $A$ were chosen to be $\Lambda_3$, and $R = \mathbf{I}$.

a

$$A_2 = \begin{pmatrix} 0.628 & 0.006 - 0.125i \\ 0.006 + 0.125i & 0.622 \end{pmatrix}$$

$$|b_2\rangle = \begin{pmatrix} 0.382 + 0.603i \\ -0.572 + 0.403i \end{pmatrix}$$

b

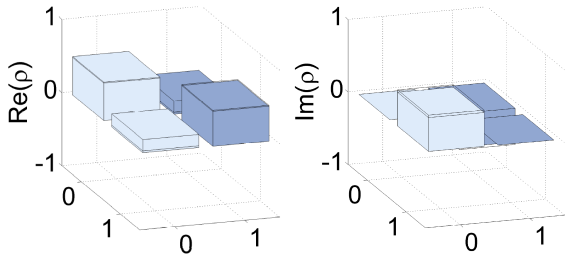


c

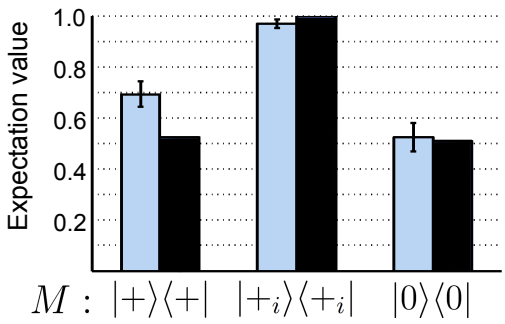


FIG. S2: Additional experimental results. **(a)** The figure shows another system of linear equations, depicted by the matrix $A_2$ as well as the state vector $|b_2\rangle$. **(b)** The reconstructed density matrix of the experimentally obtained output state $|x\rangle$ is shown. This density matrix is obtained by choosing the local operation $R_2 = R_x(\frac{89}{60}\pi).R_y(-\frac{3}{8}\pi)$ and the eigenvalues $\lambda_1 = \frac{1}{2}$ and $\lambda_2 = \frac{3}{4}$. The fidelity of the reconstructed density matrix is $0.976 \pm 0.010$. The wireframe shows the theoretical prediction. **(c)** We show the experimentally determined (blue) and theoretical (black) expectation values of several operators $\hat{M}$ where $\hat{M}$ is chosen to be the projection on the states $|0\rangle$, $|+\rangle$, and $|+_i\rangle$, respectively, with $|+\rangle = (|0\rangle + |1\rangle)/\sqrt{2}$, and $|+_i\rangle = (|0\rangle + i|1\rangle)/\sqrt{2}$.